

THE PROGENITOR OF SUPERNOVA 1993J REVISITED¹

SCHUYLER D. VAN DYK

IPAC/Caltech, Mailcode 100-22, Pasadena CA 91125
email: vandyk@ipac.caltech.edu

PETER M. GARNAVICH

Physics Department, University of Notre Dame, Notre Dame, IN 46556-5670
email: pgarnavi@miranda.phys.nd.edu

ALEXEI V. FILIPPENKO

Department of Astronomy, University of California, Berkeley, CA 94720-3411
email: alex@astro.berkeley.edu

PETER HÖFLICH

Astronomy Department, University of Texas, Austin, TX 78712
e-mail: pah@astro.as.utexas.edu

and

ROBERT P. KIRSHNER, ROBERT L. KURUCZ, AND PETER CHALLIS

Harvard-Smithsonian Center for Astrophysics, Cambridge, MA 02138
email: (rkirshner, rkurucz, pchallis)@cfa.harvard.edu

To appear in PASP (2002 Dec)

ABSTRACT

From *Hubble Space Telescope* images with $0''.05$ resolution we identify four stars brighter than $V = 25$ mag within $2''.5$ of SN 1993J in M81 which contaminated previous ground-based brightness estimates for the supernova progenitor. Correcting for the contamination, we find that the energy distribution of the progenitor is consistent with that of an early K-type supergiant star with $M_V \approx -7.0 \pm 0.4$ mag and an initial mass of 13–22 M_\odot . The brightnesses of the nearby stars are sufficient to account for the excess blue light seen from the ground in pre-explosion observations. Therefore, the SN 1993J progenitor did not necessarily have a blue companion, although by 2001, fainter blue stars are seen in close proximity to the supernova. These observations do not strongly limit the mass of a hypothetical companion. A blue dwarf star with a mass up to 30 M_\odot could have been orbiting the progenitor without being detected in the ground-based images. Explosion models and observations show that the SN 1993J progenitor had a helium-rich envelope. To test whether the helium abundance could influence the energy distribution of the progenitor, we calculated model supergiant atmospheres with a range of plausible helium abundances. The models show that the pre-supernova colors are not strongly affected by the helium abundance longward of 4000 Å, and abundances ranging between solar and 90% helium (by number) are all consistent with the observations.

Subject headings: supernovae: general—supernovae: individual (SN 1993J)—galaxies: individual (M81, NGC 3031)—stars: evolution

1. INTRODUCTION

Direct identification of the progenitor star has been scarce for the more than 2000 known historical supernovae (SNe); hence, our knowledge of the types of stars that become SNe is based primarily on models of stellar evolution and observations of the environments in which SNe occur. Pre-SN stars have been detected for only five events: SN 1987A in the LMC (e.g., Walborn et al. 1987), SN 1961V in NGC 1058 (Goodrich et al. 1989; Filippenko et al. 1995), SN 1978K in NGC 1313 (Ryder et al. 1993), SN 1997bs in NGC 3627 (Van Dyk et al. 1999), and SN 1993J in M81 (Filippenko 1993a; Aldering, Humphreys, & Richmond 1994, hereafter AHR; Cohen, Darling, & Porter 1995). Interestingly, the properties of all five of these SNe are atypical of type II supernovae (SNe II). In fact, the highly unusual properties of SN 1961V and SN 1997bs (Van Dyk et al. 2000) suggest that

they were actually eruptions of extremely massive stars, similar to η Carinae, rather than genuine SNe.

SN 1993J was initially classified as a SN II, because its optical spectra showed hydrogen lines (Filippenko 1993b; Garnavich & Ann 1993), but it soon developed the characteristics of a SN Ib (Filippenko & Matheson 1993; Filippenko, Matheson, & Ho 1993; Filippenko, Matheson, & Barth 1994) — hence, the classification as Type IIb. Several groups (see the review by Wheeler & Filippenko 1996) concluded that the progenitor of SN 1993J was a massive star (10–20 M_\odot) that had lost most of its hydrogen envelope before exploding. The models generally employ a close companion star to strip the progenitor of its envelope, since mass loss through a wind is not efficient at such low initial masses. The companion gains mass and may reach more than 15 M_\odot before the supernova explosion (Woosley et al. 1994). Höflich, Langer, & Duschinger (1993) offered

¹BASED ON OBSERVATIONS MADE WITH THE NASA/ESA *HUBBLE SPACE TELESCOPE*, OBTAINED IN PART FROM THE DATA ARCHIVE OF THE SPACE TELESCOPE SCIENCE INSTITUTE, WHICH IS OPERATED BY THE ASSOCIATION OF UNIVERSITIES FOR RESEARCH IN ASTRONOMY, INC., UNDER NASA CONTRACT NAS 5-26555.

an alternative model, in which a single, very massive star loses its envelope through a wind before exploding; the results, however, do not fit the observations as well as do binary star models.

The photometric properties of the SN 1993J progenitor were estimated by AHR, using an extensive ground-based photographic and CCD archive for M81. Their analysis was affected by the range in quality of the observations and the crowded field near the SN. AHR concluded that the progenitor was a K0 supergiant with contamination from one or more blue stars projected near the SN and possibly light from an OB association that spawned SN 1993J.

From a set of CCD images obtained in the 1980s to search for novae in M81, Cohen et al. (1995) determined that the SN 1993J progenitor was not variable at the 0.2 mag level. They also confirmed the AHR estimate of the progenitor color. Crofts (1995) obtained high-quality CCD images 600 days after maximum brightness and found a red star with $I \approx 22.7$ mag within $1''$ of SN 1993J. This star was responsible for the elliptical appearance of the progenitor in the AHR set of images, even under good seeing conditions.

In the course of the Supernova Intensive Study (SINS) collaboration, multiwavelength *Hubble Space Telescope* (*HST*) images had been obtained of SN 1993J and the surrounding star field in 1994 and 1995, while the SN was fading. The SN and the field have also been observed in 2001, though not as the main target, by program GO-9073 (see Liu, Bregman, & Seitzer 2002). In this paper, we use all these data to help resolve some questions that were raised by the ground-based data about the progenitor. In particular, we estimate the contamination of the progenitor light by stars which are unresolved in the ground-based images and attempt to determine the source of the excess blue light seen by AHR. We also estimate the brightness, color, age, and initial mass of the progenitor. In §2 we describe the observations and photometric reduction. The implications of the *HST* data for the pre-SN observations are discussed in §3, and conclusions are presented in §4.

2. OBSERVATIONS AND DATA REDUCTION

Short exposures were obtained, when the SN was still fairly bright, on 1994 April 18 (UT is used throughout this paper) with the *HST* WFPC2 through filters F336W, F439W, F555W, F675W, and F814W, which approximate standard Johnson-Cousins *UBVRI* bandpasses. After the SN faded further, images were obtained on 1995 January 31 through the same filters, and additionally, the UV filter F255W. Exposures through filters F450W, F555W, and F814W were also obtained by GO-9073 on 2001 June 4. Table 1 summarizes all of the *HST* observations.

Photometry of these images was performed using HSTphot version 1.1 (Dolphin 2000a,b). This package automatically accounts for WFPC2 point-spread function (PSF) variations and charge-transfer effects across the chips, zero-points, aperture corrections, etc., and returns *UBVRI* magnitudes as output. HSTphot appears to have a limiting (image-to-image) photometric accuracy of ~ 0.02 mag (Dolphin 2000a). The transformations, even at faint magnitudes, should be at this level or better (Dolphin 2000b).

Approximately 25 stellar sources are within $2''.5$ of the SN that can be identified in the sum of all images obtained in 1995 (see Figure 1). Of these, only six have $B < 25$ mag, and only four have $V < 25$ mag. For identification purposes, the angular distances and position angles from SN 1993J for stars A–F have been listed in Table 2. The magnitudes from each epoch, along with the adopted magnitudes for the stars in the SN environment (the uncertainty-weighted average of the three epochs), are given in Table 2. Measurements for the brightness of SN 1993J itself are given in Table 3.

A distance to M81 of 3.63 ± 0.34 Mpc ($\mu = 27.80 \pm 0.20$ mag) has been determined from *HST* observations of Cepheid variables (Freedman et al. 1994). The reddening to SN 1993J is not well-determined. Richmond et al. (1994) estimate $E(B - V) = 0.08\text{--}0.32$ mag. From early-time spectra, Clocchiatti et al. (1995) find a visual extinction $A_V = 0.74 \pm 0.05$ mag. As AHR point out, the range in likely A_V to the SN is about 0–1.5 mag. We adopt $A_V = 0.75$ mag, in agreement with Clocchiatti et al. (1995) and consistent with the midrange of colors and magnitudes of stars in the SN's environment (see below). Therefore, a star with $B = 25$ mag, if physically associated with M81, would have absolute magnitude $M_B \approx -3.6$.

The SN was still bright in 1995 January ($V \approx 18.8$ mag) and faint stars closer than $\sim 0''.25$ (~ 4.4 pc at the distance of M81) would not be resolved, if present. Stars with $B > 25$ mag, even in 2001, are more than 11 times fainter in B than the estimated brightness of the progenitor (see below) and could not substantially affect the progenitor photometry.

The position of the red star reported by Crofts (1995; his estimates are $\delta\theta = 0''.84$, P.A. = 344°) is consistent with Star A in the *HST* images. However, Crofts' measurement for the star, $I \approx 22.7$ mag, is ~ 2 mag fainter than our *HST* measurement of 20.7 mag. Also, the color for this star, $R - I = 1.14$ mag, based on the *HST* measurements, is much redder than the $R - I \approx 0.5$ mag reported by Crofts. Star A may be somewhat variable, as seen from the magnitudes derived from all three epochs of *HST* observations. On the other hand, the variability is certainly not of this degree, nor can we easily explain the difference due to bandpass differences. This discrepancy demonstrates the difficulty in obtaining accurate photometry of closely blended stars, even from the best ground-based sites.

3. DISCUSSION

Analysis of archival ground-based images by AHR showed that no single star could fit the progenitor's energy distribution. They suggested that the spectrum is best fit by a slightly reddened K0 supergiant, plus light from an OB association surrounding the SN. From the *HST* images, we find four stars, A–D, with $V \lesssim 24$ mag, that fall within the resolution element of observations typical for AHR (FWHM $\approx 1''.5$, corresponding to FWZI $\approx 2''.5$), which may have influenced flux measurements of the progenitor by AHR. Star A appears to be variable in all bands, which might possibly have influenced the progenitor flux measurements by Cohen et al. (1995). However, they rule out variability for the progenitor at the ~ 0.2 mag level; the variability we measure in V for Star A is comparable to, or

slightly larger than, this level, although the measured behavior here is consistent with that shown by Cohen et al. (We note that the apparent variability for Star A we measure in B and R is > 0.2 mag.) Two blue stars are seen in Figure 1 very close to the SN, but they are near the limit of the detection threshold and are therefore likely too faint to substantially affect the progenitor photometry. The $V = 23.5$ mag star just east of due north and the $V = 24.3$ mag, somewhat extended, source to the southwest, both near the edge of the circle in the figure, are well in the wings of the typical ground-based seeing disk. All other stars within the circle are quite faint ($V \approx 25$ – 26 mag).

Based on a visual inspection of the *HST* images, SN 1993J does not appear to be a member of a cluster or association. Using IRAF²/DAOFIND, a detailed comparison between the density of stars within $2''$ of the SN with the overall star density on the B -band frames also does not indicate a statistically significant stellar clustering around the supernova. SN 1993J is at a large radial distance from the center of M81 ($4'.8$), located along an outer spiral arm, which is interspersed with dust lanes. Nonetheless, the photometry indicates that recent star formation has occurred in the SN environment.

Figure 2 shows the color-color diagrams for the environment. The $(U - B)$ vs. $(B - V)$ diagram serves as the best diagnostic of the reddening and extinction in the SN's neighborhood, which, within the uncertainties in the stellar photometry, is $A_V = 0$ – 1.5 mag, with the mid-value $A_V = 0.75$ mag [$E(B - V) = 0.24$ mag, assuming a Cardelli, Clayton, & Mathis (1989) reddening law]. This is consistent with the locus of most of the stars on this diagram. We adopt this midvalue, although the reddening in the environment appears to be variable and may at some locations exceed this value, up to $A_V \approx 2$ mag. Figure 3 shows the color-magnitude diagrams for the environment. The brightest blue star on the diagrams is, of course, SN 1993J, which clearly has unusual colors, due to its emission-line spectrum. From these diagrams, Stars C and D are consistent with late O-type to early B-type, likely on the main sequence (other possible fainter, young main-sequence stars are also seen in the environment). Star A is quite red and is consistent with a K-type supergiant, while, from Figures 3a and 3b, Star B is either more evolved than Stars C and D or is experiencing greater reddening. The detected fainter stars, with $V > 24.5$ mag, tend to be red, owing to the relative lack of sensitivity of the U and B bands (see Table 1).

The spectral energy distributions for Stars A–D are compared with that observed for the SN 1993J progenitor in Figure 4. The archival images used by AHR were taken under a wide range of conditions, but, even for those obtained under the best conditions, the magnitude estimate for the progenitor still contained some or all of the light from these four stars. Star A contributed $\sim 25\%$ of the I -band flux measured by AHR for the progenitor, but a negligible amount of blue light. The three other stars, B–D, contributed very little red light, but together contributed nearly 80% of the blue light and may be the source of the apparent excess flux at short wavelengths. One concern

might be that background subtraction performed by AHR as part of the measurement process for the ground-based images already accounts for the mean contribution of these stars in an aperture, since the spatial distribution of stars within the aperture is similar to the distribution of stars in the overall background (due to the lack of a well-defined OB association around the progenitor). However, presuming that the mode is used to estimate the aperture photometry background in a sky annulus outside of the aperture, the fainter pixels in an image are given greater weight than the brighter ones concentrated in resolved stars. (Besides, AHR preferred PSF-fitting over aperture photometry in their measurements.) Therefore, the nearby stars would still contaminate the PSF of the progenitor star measured from the ground.

To determine the likely energy distribution of the SN 1993J progenitor we must correct the AHR distribution for this contamination, limits for which are shown in Figure 5. The sum of the light from the four stars is computed with (1) equal weight (dotted line) and (2) following a possibly more realistic case, in which the contaminating star contribution declines with angular distance from the progenitor (dot-dashed line). Because the central part of a ground-based PSF is similar to a Gaussian, the degree of contamination is likely to decline with distance in a similar manner. To weight the contribution from Stars A–D we use a Gaussian distribution, which is the sum of the unit-weight central distribution of the progenitor light and the distribution of the light from the contaminating star,

$$F_\lambda = \sum_{i=A\dots D} F_{\lambda i} e^{-r_i^2/4\sigma^2},$$

where r_i is the distance of the contaminating star from the progenitor and σ is the width of the distribution [abbreviated “ $\Sigma(F^*g)$ ” in Figure 5]. Since, for a Gaussian, the FWHM = 2.35σ , and the FWHM is a function of wavelength, σ is also wavelength-dependent. From the AHR observational data, excluding the V and R measurements of Perelmuter (1993; AHR note that these measurements are several σ above the mean in these bands), the values for σ , weighted by the standard deviations in the measurements, are $\sigma_U = 0''.85$, $\sigma_B = 0''.61$, $\sigma_V = 0''.69$, $\sigma_R = 0''.77$, and $\sigma_I = 0''.53$. The corrected progenitor energy distributions are shown in Figure 5 as the long-dashed line (equal weight) and the short-dashed line (Gaussian weight).

The actual energy distribution of the progenitor star probably falls somewhere within these limits. In the ultraviolet (UV) the total flux from the surrounding stars is likely $\sim 1\sigma$ from the AHR U -band flux. Thus, within the errors, the blue stars near the SN could account for all the UV flux of the progenitor measured by AHR, and the corrected U -band flux from the progenitor is essentially undetermined. To possibly better estimate the progenitor's energy distribution at redder bands, we simulated the light of the progenitor, plus the contamination from the nearby stars, as would be measured from the ground.

We did this by first subtracting the SN PSF from the 2001 *HST* F450W (B), F555W (V), and F814W (I) images (when the SN was the faintest), employing a TinyTim model PSF (Krist 1995) in each band and the routines

²IRAF (Image Reduction and Analysis Facility) is distributed by the National Optical Astronomy Observatories, which are operated by the Association of Universities for Research in Astronomy, Inc., under cooperative agreement with the National Science Foundation.

ALLSTAR and SUBSTAR (Stetson 1987, 1992) within IRAF/DAOPHOT. We then added at the SN position a fake star, representing the progenitor, using ADDSTAR within IRAF/DAOPHOT. We did this in a series of fake star trials, with a range of different input apparent magnitudes. These trial images were then convolved with a two-dimensional Gaussian with the wavelength-dependent values of σ above, to simulate ground-based observing conditions. (These convolved images also then contained the light of the contaminating stars.) The model PSF was also convolved with the same Gaussian and subsequently applied to each of the convolved trial images in ALLSTAR, to obtain magnitudes for each of the fake star trials in each band. We then determined which convolved fake progenitor magnitude best matched that measured by AHR in each band for the actual progenitor. The input magnitude which resulted in this best match likely provided the best estimate of the actual progenitor’s brightness in each band.

We show in Figures 6a–6c the input fake, or hypothetical, progenitor images, before convolution, which resulted in the best matches to the AHR magnitudes after convolution. [Note the presence of the light echo (Liu et al. 2002; Sugerman & Crotts 2002), particularly in the F450W and F555W images.] The resulting magnitude estimates for a hypothetical progenitor star are $B \approx 22.4$, $V \approx 21.6$, and $I \approx 19.7$ mag. In the F450W image the faint, very nearby Stars E and F are only $\sim 1/4$ the hypothetical progenitor star’s brightness (some negative pixels resulting from oversubtraction of the SN are also seen). The fake progenitor in the I band has nearly the same brightness as the SN itself in the 2001 F814W image and is only ~ 1 mag brighter than Star A. In a sense, these final trial images simulate pre-SN WFPC2 images, had it been possible for them to have been obtained.

We show in Figure 7a the final Gaussian-convolved fake progenitor image for F814W (I) as an example (compare this with Figure 6c). In general, the final test images in all three bands closely resemble the ground-based images shown by AHR (their Figure 1). Note the elliptical shape of the fake progenitor in the convolved I -band image, due primarily to the presence of Star A. (For the I -band trials, Star A dominated the resulting convolved stellar profile for a faint fake progenitor, but the profile resolved into two stars as the trials were increased in brightness.) We show in Figure 7b the output image from ALLSTAR, with the fake progenitor subtracted. Star A becomes far more obvious after subtraction, although this star, as well as Stars B–D (which are much fainter at I), are all within the seeing disk of the convolved fake progenitor. (Compare Figure 7b with Figure 1 in AHR; their PSF-subtracted I -band image, with the progenitor removed, clearly shows the presence of an object which we suspect is Star A.) Our simulation demonstrates that the ground-based measurements, even under good seeing conditions, contained not only the light of the progenitor star, but also that of the nearby contaminating stars.

The formal uncertainties in the magnitude estimates for the progenitor, mostly due to aperture effects, small PSF mismatches, slight PSF oversubtraction, small disagreements between HSTphot and DAOPHOT results, and transformations to standard magnitudes, are estimated to

be ~ 0.30 mag in each band. We have estimated that variable seeing in B and V (corresponding to the range in seeing for the data in AHR) leads to an additional uncertainty of ~ 0.1 mag. Furthermore, the uncertainties in the V and, particularly, B magnitudes could be somewhat larger, since the faint stars E and F (and possibly others) very close to the progenitor are comparable to the progenitor’s brightness. Moreover, the relatively blue light echo (Liu et al. 2002; Sugerman & Crotts 2002), although faint and almost $2''$ from the SN, may contaminate the convolved fake progenitor’s brightness in B and V to some extent. The magnitude estimates are shown in Figures 3 and 5. To within the uncertainties, the simulated magnitudes agree fairly well with the limits shown in Figure 5, although the consistency is somewhat better in B and I than in V .

Also shown in Figure 3 are solar-metallicity isochrones from Bertelli et al. (1994) for 8 Myr and 16 Myr, reddened by $E(B - V) = 0.24$ mag and adjusted for the M81 distance. The 16 Myr isochrone fits reasonably well the locus of Star A. If we assume that the SN progenitor and Star A were coeval, this age provides at least a lower limit to the progenitor’s mass, as 16 Myr is roughly the main-sequence lifetime of an $12\text{--}14 M_{\odot}$ star (Schaller et al. 1992; Bertelli et al. 1994). With this assumption, we would expect that the SN progenitor was at least as massive as Star A, since Star A is likely a red supergiant and therefore also will likely explode as a supernova. The locus of the fake progenitor star on the diagrams is reasonably well fit, particularly in the red, by the 8 Myr isochrone, which is roughly the main-sequence lifetime of a $21\text{--}24 M_{\odot}$ star. However, in the blue, the fake progenitor is somewhat better fit by the blue loop of the 16 Myr isochrones (again, the actual uncertainties in B and V for the fake progenitor are likely larger than the formal uncertainties). Bluer colors for the progenitor would agree with the evidence that the progenitor lost most of its hydrogen envelope (Filippenko et al. 1994) and with a possible transition from red to blue supergiant during the late stages of the progenitor evolution (e.g., Immler, Aschenbach, & Wang 2001).

Additionally, we can assign an approximate spectral type and luminosity class to the uncontaminated energy distribution for the progenitor, through construction of model atmospheres for supergiants using the ATLAS12 code (Kurucz 1993). One can see that the model colors for an early K-type (K0) supergiant agree reasonably well with the overall distribution. Because the progenitor lost most of its hydrogen envelope (e.g., Filippenko et al. 1994) and the progenitor atmosphere was helium-rich (e.g., Garnavich & Ann 1994), we have calculated the K0 I broadband colors for three helium abundances: solar, 75% helium, and 90% helium (by number). As expected, the colors for the solar-abundance model are very close to those given by Bessell (1990) from the Vilnius spectra. Unfortunately, the three models primarily differ in the UV, where the corrected energy distribution of the progenitor is relatively undetermined. At longer wavelengths the colors of all three K0 I star models are in good agreement with the probable energy distribution of the progenitor.

Finally, after accounting for the contamination by nearby stars, we can place a limit on the brightness of any blue companion to the SN 1993J progenitor. The models

show that the K0 I progenitor had $U \approx 24$ mag, thus contributing very little to the flux measured by AHR in that band. A close hypothetical progenitor companion with $U < 22.4$ mag, added to the light from Stars A–D, would cause the total UV flux to exceed the AHR measurement for the progenitor by $\sim 1\sigma$. Conservatively, any progenitor companion could not have been brighter than $U = 22.0$ mag and still be consistent with those measurements. The AHR uncertainty in the B band is small, so adding an additional star of $B < 23.0$ mag to the ones accounted for here would exceed the observed flux by $\sim 2\sigma$ for a K0 I progenitor. Thus, the progenitor companion must have been less luminous than $M_B \approx -5.6$ mag, assuming $A_V = 0.75$ mag. Since O6 V and later-type dwarfs have $M_B > -5.4$ mag ($M_V > -5.0$ mag; Humphreys & McElroy 1984) and masses of up to $30 M_\odot$, we find that any hypothetical companion actually could have been of very high mass and still remained undetected.

4. CONCLUSIONS

We have used *HST* images of SN 1993J after outburst to search for stars within a ground-based resolution element, which may have contaminated the archival ground-based observations of the SN progenitor. We find four stars within $2''5$ of the progenitor which were at least partially included in the progenitor energy distribution determined by AHR. Correcting for this contamination we find the following.

- 1) The progenitor may have had apparent $V = 21.6 \pm 0.3$, $B - V = 0.8 \pm 0.6$, and $V - I = 1.9 \pm 0.5$ mag, implying an absolute magnitude $M_V \approx -7.0 \pm 0.4$ for $A_V = 0.75$ mag (the uncertainty in the absolute magnitude includes the estimated photometric uncertainty, plus the uncertainty in the distance modulus). The brightness and colors are consistent with those of a reddened early K-type supergiant, although possibly somewhat too blue in the blue bands. The mass of the progenitor can be constrained by the possible mass for the nearby red supergiant, Star A, i.e., $\sim 13 M_\odot$, and the age and mass of a hypothetical progenitor suggested by its brightness and colors, i.e., $\sim 22 M_\odot$. This range, $13\text{--}22 M_\odot$, is consistent with other estimates for the progenitor mass in the literature (e.g., Podsiadlowski

et al. 1993; Woosley et al. 1994; Young, Baron, & Branch 1995; Iwamoto et al. 1997).

- 2) Model atmospheres with a wide range of helium abundances fit the observed progenitor energy distribution redward of 4000 \AA . Although at shorter wavelengths the models show a greater spread in color with helium fraction, the data are insufficient to differentiate between them.
- 3) The blue excess seen by AHR can be fully accounted for by the nearby stars. The progenitor was not a member of a significant OB association. Any companion to the progenitor must have had $M_B > -5.6$ mag for reasonable assumptions of the reddening and distance to the SN. The mass of the companion is not very strongly constrained, but must be less than $30 M_\odot$. This is consistent with the binary mass-transfer scenario, even for conservative mass exchange (e.g., Podsiadlowski et al. 1993).

SN 1993J appears to be interacting with circumstellar material ejected by the progenitor during its evolution (e.g., Filippenko et al. 1994; Van Dyk et al. 1994; Patat, Chugai, & Mazzali 1995; Matheson et al. 2000). The energy from this interaction continues to power the optical light curve, which in 1995 slowed its decline to less than $2 \text{ millimag d}^{-1}$ (Garnavich et al. 1995). Comparing the magnitudes derived from the *HST* WFPC2 images in 1995 and 2001, the SN is still declining at only $\sim 0.2 \text{ mag yr}^{-1}$. Recent ACS multi-band images have been obtained with *HST* by program GO-9353, but even with the superior sensitivity and resolution of ACS, the SN is likely still too bright to successfully isolate a companion or other stars in the immediate SN environment ($\leq 0''.1\text{--}0''.2$). Only when the SN sufficiently fades, probably not for a few more *HST* cycles, can the high-resolution imaging be used to search for a companion to the SN progenitor and better determine the progenitor's nature.

This work was supported in part by NASA through grants GO-2563, GO-8648, GO-9114, and AR-8754 from the Space Telescope Science Institute, which is operated by the Association of Universities for Research in Astronomy, Inc., under NASA contract NAS 5-26555. We thank Greg Aldering for comments that helped improve this paper.

REFERENCES

- Aldering, G., Humphreys, R. M., & Richmond, M. W. 1994, *AJ*, 107, 662 (AHR)
- Bertelli, G., Bressan, A., Chiosi, C., Fagotto, F., & Nasi, E. 1994, *A&AS*, 106, 275
- Bessell, M. S. 1990, *PASP*, 102, 1181
- Cardelli, J. A., Clayton, G. C., & Mathis, J. S. 1989, *ApJ*, 345, 245
- Clocchiatti, A., Wheeler, J. C., Barker, E. S., Filippenko, A. V., Matheson, T., & Liebert, J. W. 1995, *ApJ*, 446, 167
- Cohen, J. G., Darling, J., & Porter, A. 1995, *AJ*, 110, 308
- Crotts, A. P. S. 1995, *IAU Circ.* 6132
- Dolphin, A. E. 2000a, *PASP*, 112, 1383
- Dolphin, A. E. 2000b, *PASP*, 112, 1397
- Filippenko, A. V. 1993a, *IAU Circ.* 5737
- Filippenko, A. V. 1993b, *IAU Circ.* 5740
- Filippenko, A. V., Barth, A. J., Bower, G. C., Ho, L. C., Stringfellow, G. S., Goodrich, R. W., & Porter, A. C. 1995, *AJ*, 110, 2261 (Erratum: 1996, 112, 806)
- Filippenko, A. V., Matheson, T., & Barth, A. J. 1994, *AJ*, 108, 2220
- Filippenko, A. V., Matheson, T., & Ho, L. C. 1993, *ApJ*, 415, L103
- Freedman, W. L., et al. 1994, *ApJ*, 427, 628
- Garnavich, P., & Ann, H. B. 1993, *IAU Circ.* 5731
- Garnavich, P. M., & Ann, H. B. 1994, *AJ*, 108, 1002
- Garnavich, P., Challis, P., Kirshner, R., & Wells, L. 1995, *IAU Circ.* 6257
- Goodrich, R. W., Stringfellow, G. S., Penrod, G. D., & Filippenko, A. V. 1989, *ApJ*, 342, 958
- Höflich, P., Langer, N., & Duschinger, M. 1993, *A&A*, 275, L29
- Humphreys, R. M., & McElroy, D. B. 1984, *ApJ*, 284, 565
- Immler, S., Aschenbach, B., & Wang, Q. D. 2001, *ApJ*, 561, L107
- Iwamoto, K., Young, T. R., Nakasato, N., Shigeyama, T., Nomoto, K., Hachisu, I., & Saio, H. 1997, *ApJ*, 477, 865
- Krist, J. 1995, in *Calibrating Hubble Space Telescope: Post Servicing Mission* (Baltimore: STScI), 311
- Kurucz, R. L. 1993, in *Peculiar Versus Normal Phenomena in A-Type and Related Stars*, ed. M. M. Dworetzky, F. Castelli, & R. Faraggiana (San Francisco: ASP), 87
- Liu, J.-F., Bregman, J. N., & Seitzer, P. 2002, *ApJ*, submitted (astro-ph/0206070)

- Matheson, T., Filippenko, A. V., Ho, L. C., Barth, A. J., & Leonard, D. C. 2000, *AJ*, 120, 1499
- Patat, F., Chugai, N., & Mazzali, P. A. 1995, *A&A*, 299, 715
- Perelmuter, J.-M. 1993, *IAU Circ.* 5736
- Podsiadlowski, P., Hsu, J. J. L., Joss, P. C., & Ross, R. R. 1993, *Nature*, 364, 509
- Richmond, M. W., Treffers, R. R., Filippenko, A. V., Paik, Y., Leibundgut, B., Schulman, E., & Cox, C. V. 1994, *AJ*, 107, 1022
- Ryder, S., Staveley-Smith, L., Dopita, M., Petre, R., Colbert, E., Malin, D., & Schlegel, E. 1993, *ApJ*, 416, 167
- Schaller, G., Schaerer, D., Meynet, G., & Maeder, A. 1992, *A&AS*, 96, 269
- Stetson, P. B. 1987, *PASP*, 99, 191
- Stetson, P. B. 1992, in *ADASS* (ASP Conf. Ser. 25), ed. D. M. Worrall, C. Bimesderfer, & J. Barnes (San Francisco: ASP), 297
- Sugerman, B. E. K., & Crofts, A. P. S. 2002, *ApJL*, submitted (astro-ph/0207497)
- Van Dyk, S. D., Peng, C. Y., Barth, A. J., & Filippenko, A. V. 1999, *AJ*, 118, 2331
- Van Dyk, S. D., Peng, C. Y., King, J. Y., Filippenko, A. V., Treffers, R. R., Li, W.-D., & Richmond, M. W. 2000, *PASP*, 112, 1532
- Van Dyk, S. D., Weiler, K. W., Sramek, R. A., Rupen, M. P., & Panagia, N. 1994, *ApJ*, 432, L115
- Walborn, N. R., Lasker, B. M., Laidler, V. G., & Chu, Y. H. 1987, *ApJ*, 321, L41
- Wheeler, J. C., & Filippenko, A. V. 1996, in *Supernovae and Supernova Remnants*, ed. R. McCray & Z. Wang (Cambridge: Cambridge Univ. Press), 241
- Woosley, S. E., Eastman, R. G., Weaver, T. A., & Pinto, P. A. 1994, *ApJ*, 429, 300
- Young, T. R., Baron, E., & Branch, D. 1995, *ApJ*, 449, L51

TABLE 1
SUMMARY OF *HST* OBSERVATIONS

Date (UT)	Band	Exp. Time (s)	$m_{\text{limit}}^{\text{a}}$ (mag)	Program
1994 Apr 18	F336W	1200	23.7	GO-5480
	F439W	600	24.5	
	F555W	300	25.5	
	F675W	300	25.0	
	F814W	300	24.5	
1995 Jan 31	F255W	2400	22.1	GO-6139
	F336W	1160	23.8	
	F439W	1200	25.4	
	F555W	900	26.6	
	F675W	900	26.1	
2001 Jun 4	F814W	900	25.5	GO-9073
	F450W	2000	26.7	
	F555W	2000	26.8	
	F814W	2000	25.2	

^aThese are the approximate *HST*phot 3σ detection limits, in magnitudes, for the PC chip (programs GO-5480 and GO-6139), and for the WF4 chip (program GO-9073). Magnitudes are given in the *HST* flight system.

TABLE 2
MEASUREMENTS OF BRIGHT STARS WITHIN 2.5'' OF SN 1993J

Star	Offset ''	P.A. ^a °	Year	<i>U</i> (F366W)	<i>B</i> (F439W) ^b	<i>V</i> (F555W)	<i>R</i> (F675W)	<i>I</i> (F814W)
A	0.73	348	1994	23.82(14)	23.84(27)	22.63(04)	21.66(03)	20.67(03)
			1995	...	24.38(18)	22.86(03)	22.03(02)	20.80(01)
			2001	...	23.80(03)	22.54(01)	...	20.60(01)
			AVE.	23.82(14):	23.82(04)	22.58(01)	21.84(03)	20.70(01)
B	1.44	184	1994	23.01(14)	23.12(11)	22.92(05)	23.05(07)	23.16(14)
			1995	22.94(14)	23.27(08)	23.02(03)	23.12(04)	23.06(05)
			2001	...	23.17(02)	23.12(02)	...	22.84(10)
			AVE.	22.98(14)	23.17(03)	23.07(03)	23.10(05)	23.03(07)
C	1.22	353	1994	23.03(11)	23.98(22)	23.74(08)	23.67(12)	23.69(24)
			1995	22.97(12)	23.76(12)	23.78(04)	23.88(08)	23.55(09)
			2001	...	23.86(03)	23.77(03)	...	23.46(11)
			AVE.	23.00(12)	23.86(04)	23.77(04)	23.82(09)	23.53(11)
D	1.19	149	1994	22.90(10)	23.78(19)	23.80(08)	23.89(14)	24.12(29)
			1995	23.04(12)	23.78(11)	23.96(05)	24.04(08)	23.90(10)
			2001	...	23.78(03)	23.90(03)	...	24.19(14)
			AVE.	22.96(11)	23.78(04)	23.90(04)	24.00(09)	24.01(13)
E	0.32	335	1994
			1995	...	23.84(14)	24.04(10)	23.68(12)	23.82(14)
			2001	...	24.59(23)	24.32(07)
F	0.29	282	1994
			1995	24.35(34)	24.03(13)	24.87(09)	23.77(07)	23.96(11)
			2001

Note: The values in parentheses are the 1σ uncertainties in the last two digits of the magnitudes.

^aPosition angle, degrees from north through east.

^bThe 2001 observations by GO-9073 were made through the F450W, rather than the F439W, filter.

TABLE 3
HST PHOTOMETRY OF SN 1993J

Date (UT)	UV (F255W)	<i>U</i> (F366W)	<i>B</i> (F439W) ^a	<i>V</i> (F555W)	<i>R</i> (F675W)	<i>I</i> (F814W)
1994 Apr 18	...	17.98	18.22	17.78	16.99	17.21
1995 Jan 31	17.30	18.55	19.10	18.75	17.90	18.63
2001 Jun 04	20.48	20.32	...	19.75

Note: The 1σ uncertainties in the magnitudes are all ≤ 0.01 mag.

^aThe 2001 observations by GO-9073 were made through the F450W, rather than the F439W, filter.

Fig. 1.— The sum of the *HST* images obtained in 1995 through the F336W, F439W, F555W, F675W, and F814W filters, showing the environment around SN 1993J in M81. The circle centered on the supernova has a radius of $2''.5$, which is approximately the full-width near zero intensity (FWZI) of a Gaussian seeing disk with full-width at half maximum (FWHM) = $1''.5$ (typical seeing for observations analyzed by AHR). The six brightest stars in the SN environment are labelled. The four brightest, A–D, with $V < 24$ mag, most likely contaminated the ground-based measurements of the SN progenitor by AHR.

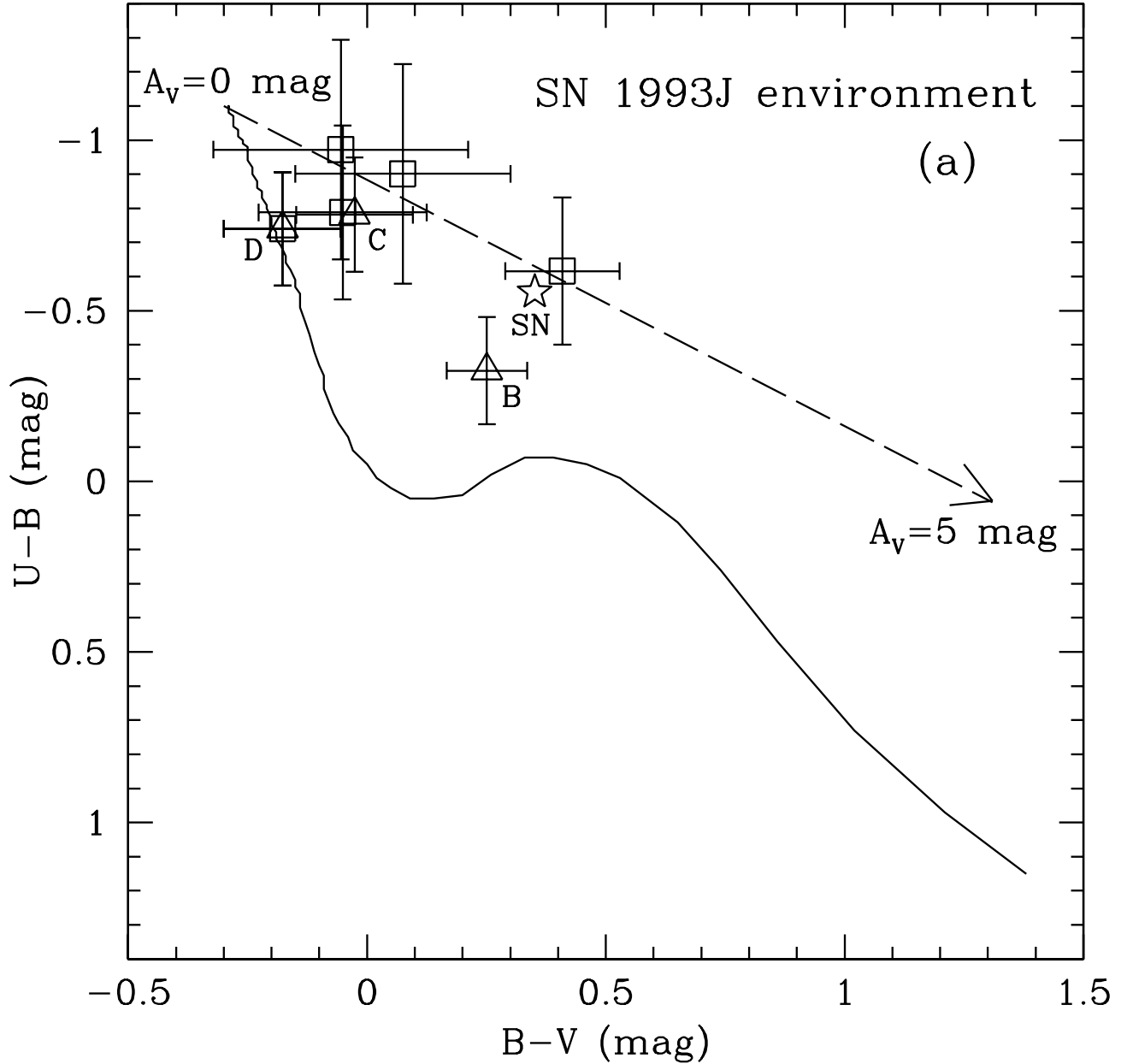


Fig. 2.— The color-color diagrams for the SN 1993J environment (an area $\sim 2''.5$ in radius, centered on the SN), measured from the 1995 *HST* images. (a) The $(U - B, B - V)$ diagram; and (b) the $(V - R, V - I)$ diagram. In both diagrams, Stars A–D are represented by *open triangles* and labelled, whereas *open squares* represent other stars in the environment. The SN (*five-pointed star*) is also labelled. In (a), Star A is not shown, due to the lack of a *U*-band measurement. In both diagrams the main-sequence locus is shown (*solid line*), as well as the reddening vector (*dashed line*), assuming a Cardelli et al. (1989) reddening law.

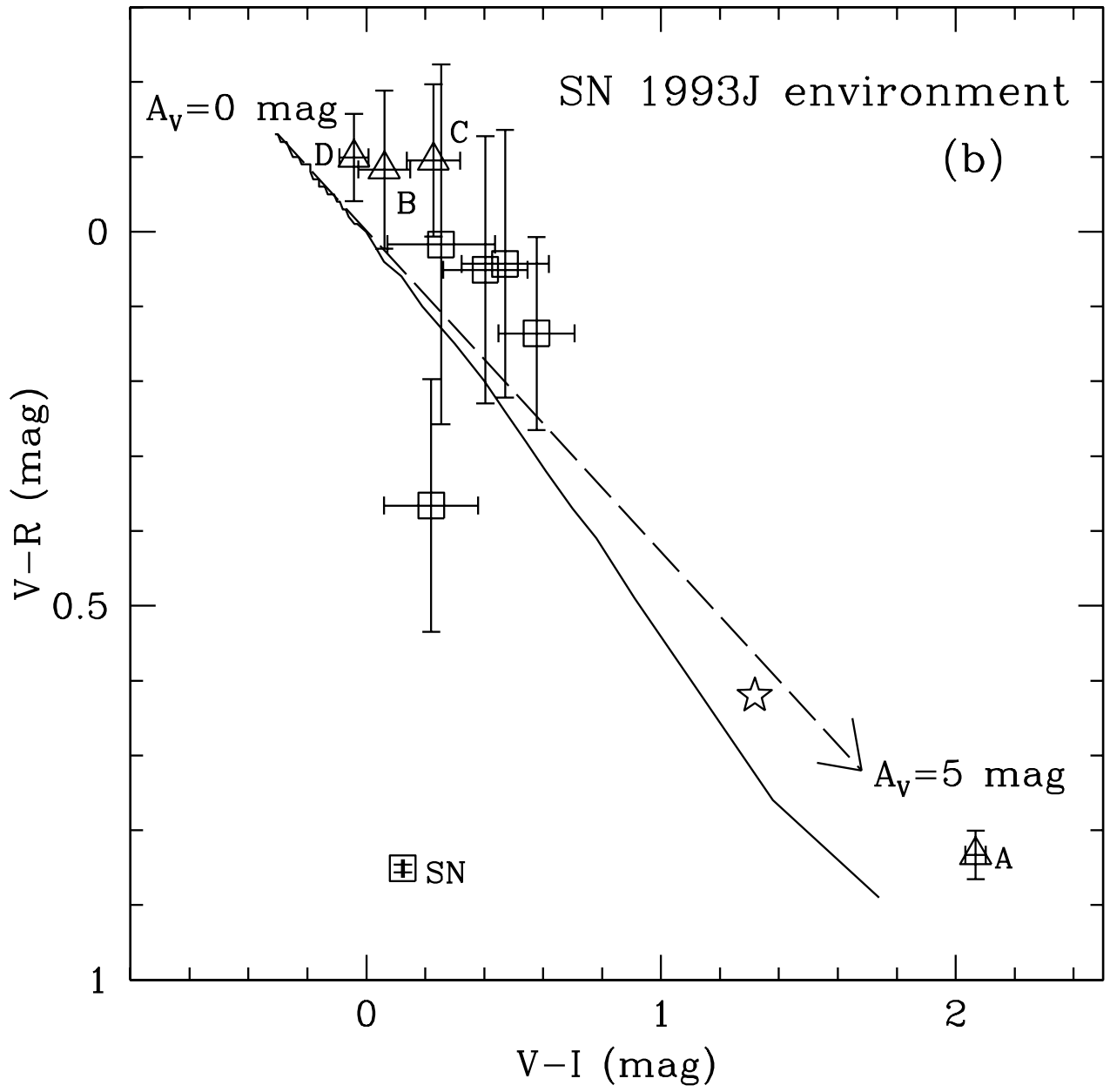


Fig. 2.— (Continued.)

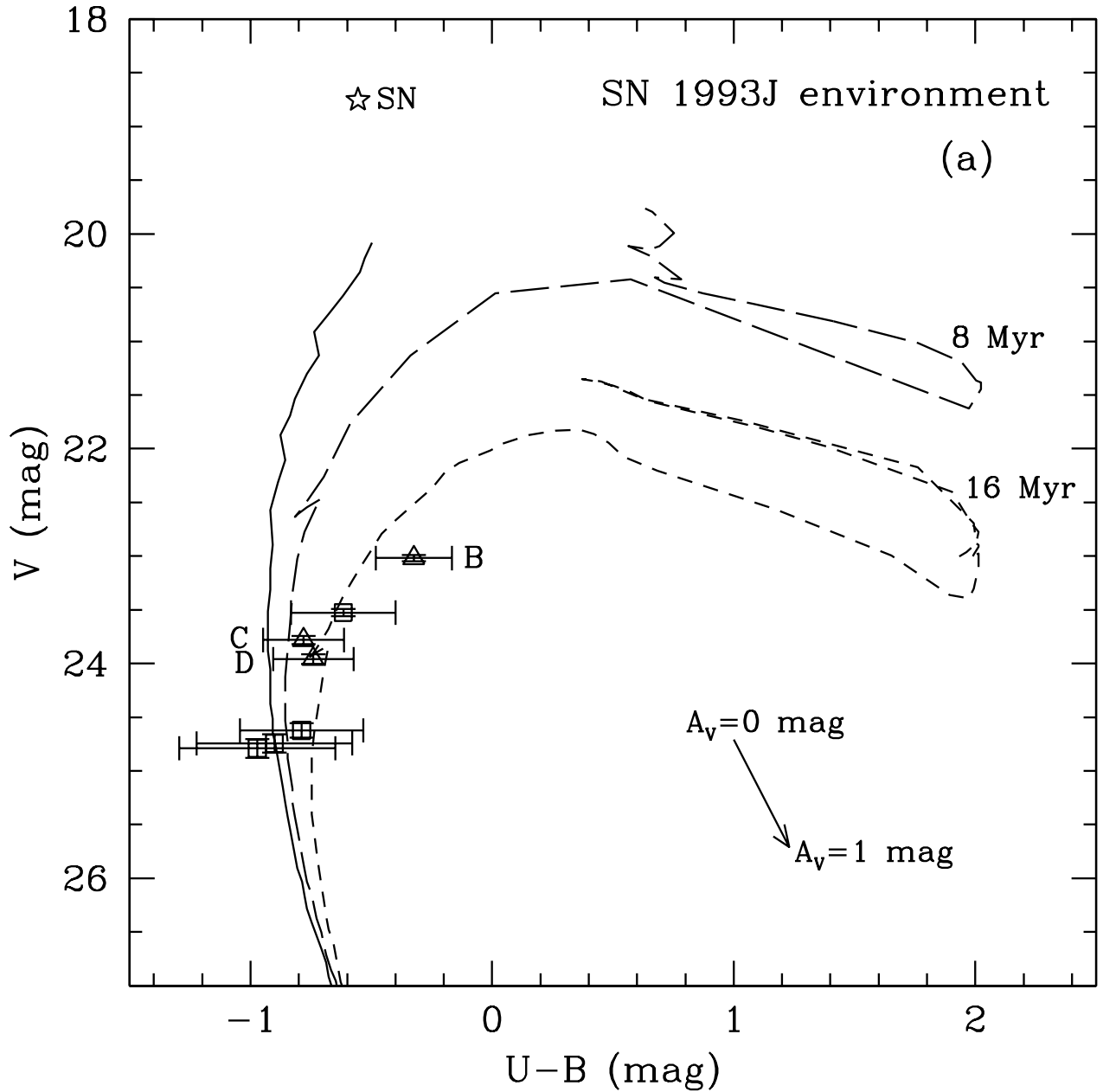


Fig. 3.— The color-magnitude diagrams for the SN 1993J environment (an area $\sim 2''.5$ radius, centered on the SN), measured from the 1995 *HST* images. (a) The $(U - B, V)$ diagram; (b) the $(B - V, V)$ diagram; and (c) the $(V - I, V)$ diagram. In all three diagrams, the *five-pointed star* with $V = 18.75$ mag is the SN, and Stars A–D are represented by *open triangles* and labelled, whereas *open squares* represent other stars in the environment. (In (a) and (b), these four other blue stars are to the north and northwest of the SN. In (c), the several faint, red stars are distributed throughout the environment. The faintest detected stars are the reddest, due to the higher sensitivity of the redder 1995 images.) The main sequence locus is the *solid track*; an 8 Myr isochrone with solar metallicity from Bertelli et al. (1994), reddened assuming $A_V = 0.75$ mag and adjusted for the M81 distance from Freedman et al. (1994), is shown as the *long-dashed track*, and a 16 Myr isochrone is shown as the *short-dashed track*. A hypothetical progenitor star is represented by the *open circle*. The reddening vector, following a Cardelli et al. (1989) reddening law, is also shown.

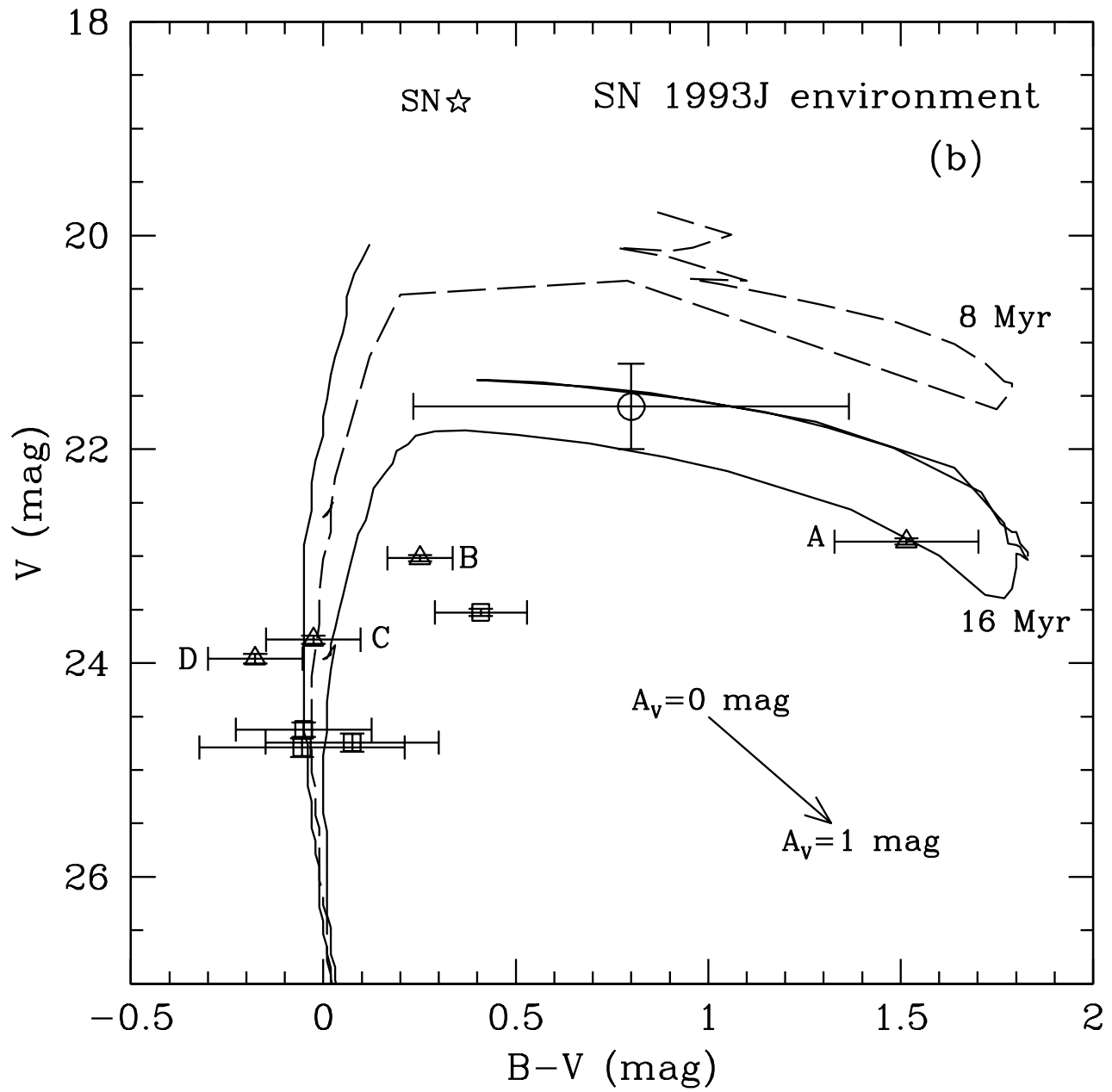


Fig. 3.— (Continued.)

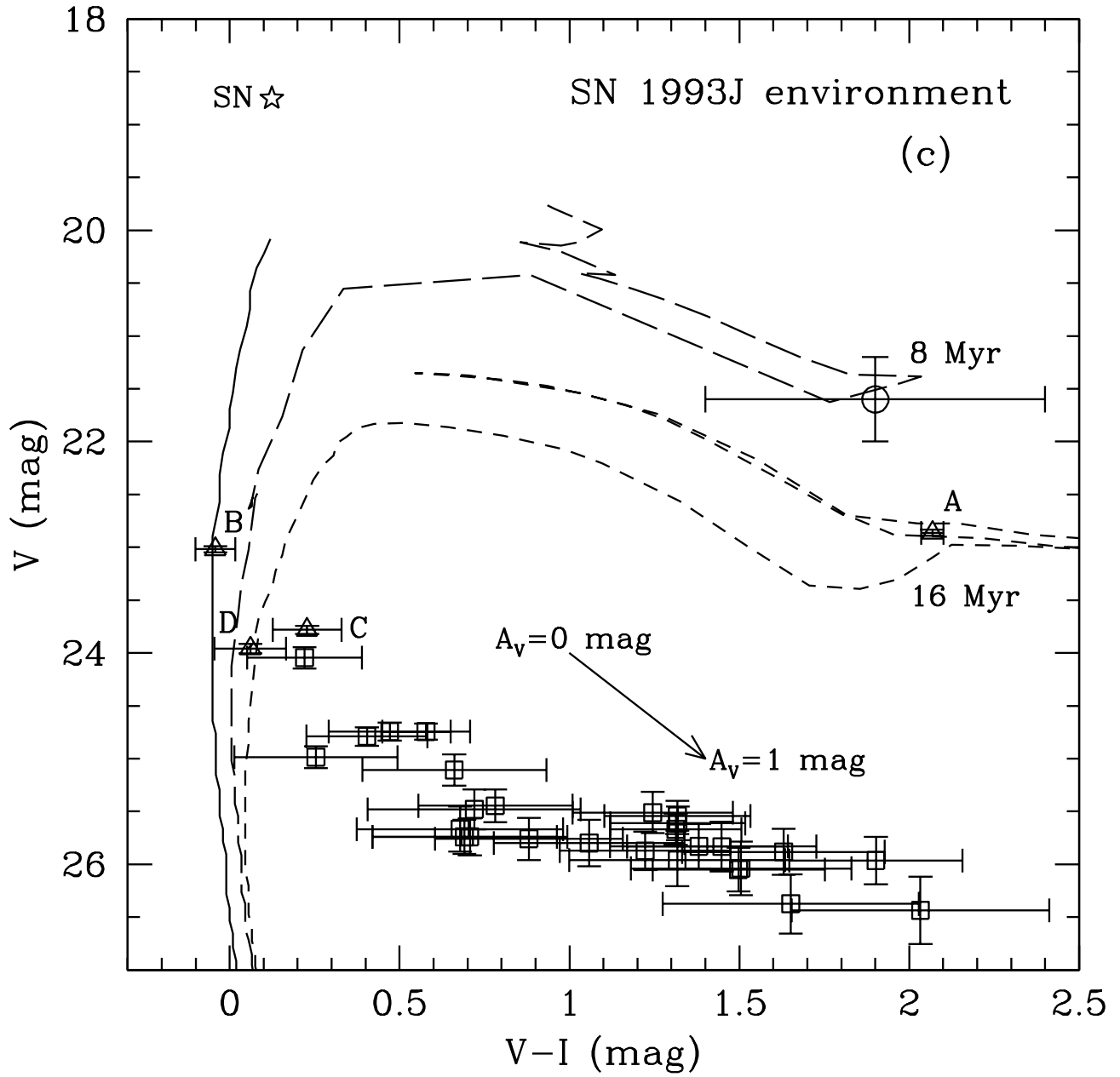


Fig. 3.— (Continued.)

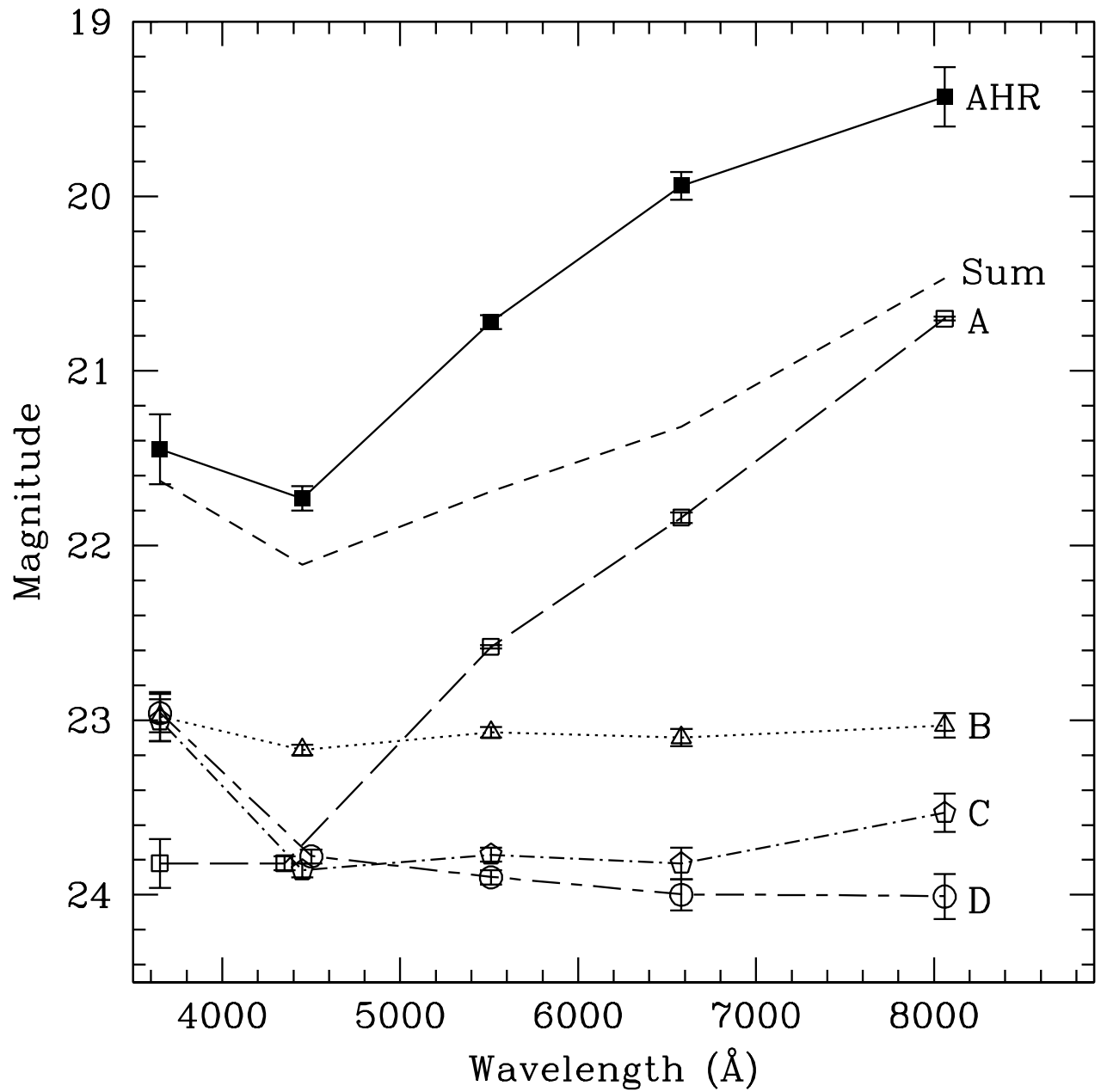


Fig. 4.— The energy distributions of the four bright stars, A–D, within $2''.5$ of SN 1993J, compared to the energy distribution for the SN progenitor from AHR. The *short-dashed line* shows the sum of all four stars.

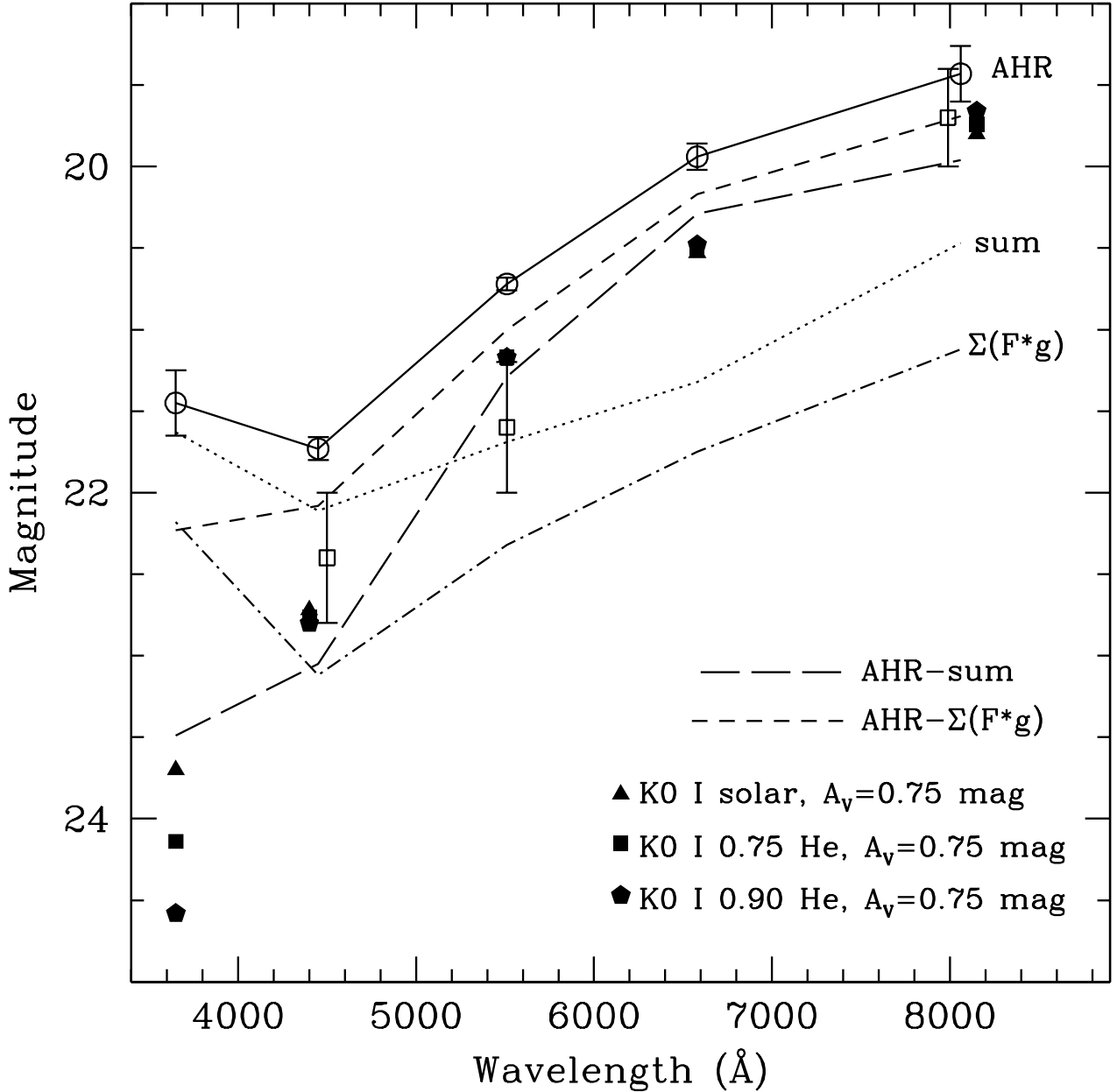


Fig. 5.— The progenitor energy distribution corrected for the contamination by the four nearby stars. The *solid line* shows the progenitor brightness from AHR, using archival ground-based observations; the *dotted line* represents the equal-weighted sum of the light from all four stars; the *dot-dashed line* represents $\Sigma(F^*g)$, the sum of the flux, F , from each of the four stars, weighted by their distance from the SN, assuming a one-dimensional Gaussian distribution, g , with wavelength-dependent width, σ (see text). The *long-dashed line* represents the progenitor energy distribution corrected by the equal-weight sum, while the *short-dashed line* represents the distribution corrected by the Gaussian-weighted sum. The former is likely a lower limit to the true progenitor spectrum, while the latter is likely an upper limit. The *open squares* represent the light from a fake, hypothetical progenitor (see text). The *solid symbols* show the energy distribution for model K-type supergiant atmospheres with a range of possible helium abundances, reddened assuming $A_V = 0.75$ mag.

Fig. 6.— (a) The F450W (*B*) *HST* image from 2001 June of the SN 1993J environment, after subtraction of the SN via fitting of a TinyTim PSF (Krist 1995) within DAOPHOT/ALLSTAR and the addition of a fake progenitor star with $B \approx 22.4$ mag. (b) The F555W (*V*) *HST* image from 2001 June, after SN subtraction and the addition of a fake progenitor star with $V \approx 21.6$ mag. (c) The F814W (*I*) *HST* image from 2001 June, after SN subtraction and the addition of a fake progenitor star with $I \approx 19.7$ mag. The light echo (Liu et al. 2002; Sugerman & Crotts 2002) is indicated in (a) and (b) by an arrow.

Fig. 7.— (a) The F814W (*I*) *HST* image from 2001 June with the fake progenitor star (see Figure 6), after convolution with a two-dimensional Gaussian with $\sigma = 0''.53$. (b) The same as (a), except after subtraction of the fake convolved progenitor via fitting of the TinyTim PSF, also convolved with the same Gaussian, within ALLSTAR. The position of Star A is indicated.

This figure "fg1.jpg" is available in "jpg" format from:

<http://arxiv.org/ps/astro-ph/0208382v1>

This figure "fg6a.jpg" is available in "jpg" format from:

<http://arxiv.org/ps/astro-ph/0208382v1>

This figure "fg6b.jpg" is available in "jpg" format from:

<http://arxiv.org/ps/astro-ph/0208382v1>

This figure "fg6c.jpg" is available in "jpg" format from:

<http://arxiv.org/ps/astro-ph/0208382v1>

This figure "fg7a.jpg" is available in "jpg" format from:

<http://arxiv.org/ps/astro-ph/0208382v1>

This figure "fg7b.jpg" is available in "jpg" format from:

<http://arxiv.org/ps/astro-ph/0208382v1>